DOI 10.59887/2073-6673.2025.18(2)-3
EDN FSMDHC

УДК 551.465

© *T. M. Maksimovskaya*[1]*, *A. V. Zimin*[1], *O. A. Atadzhanova*[1], *A. A. Konik*[1], *E. S. Egorova*[2], *D. V. Moiseev*[3], 2025
[1]Shirshov Institute of Oceanology RAS, 36 Nakhimovsky Prosp., Moscow, 117997, Russia
[2]Marine Research Center at Lomonosov Moscow State University, 1 str. 77 Leninskye Gory, Nauchny Park, Moscow, 119234, Russia
[3]Murmansk Marine Biological Institute of the Russian Academy of Sciences, 17 Vladimirskaya Str., Murmansk, 183038, Russia
*maximovskaja.t@yandex.ru

Variability of the Polar Front Characteristics in the Northwestern Barents Sea Based on In-Situ Observations from 2017 to 2023

Received 23.01.2025, Revised 27.03.2025, Accepted 10.06.2025

Abstract

This study presents oceanographic observations from the R/V Dalnie Zelentsy along the Kola Section (2017–2023), focusing on the northern Polar Front during autumn, winter, and spring. Sea ice anomalies were estimated using data from the World Data Center for Sea Ice (AARI WDC Sea-Ice). Observational data near the Marginal Ice Zone were compared with temperature and salinity fields from global oceanographic datasets, including MERCATOR PSY4QV3R1, CMEMS GLORYS12v1, and TOPAZ5. High-gradient temperature and salinity zones were observed at varying distances from the ice edge along all sections. Over the past three decades, the western Barents Sea has experienced a steady decline in sea ice cover. The northernmost Polar Front along the Kola Section ranged from 48 to 290 km from the ice edge, with temperature gradients of 0.10–0.20 °C/km and salinity gradients of 0.012–0.025 psu/km. The frontal zone width did not exceed 55 km. Among the assessed data products, MERCATOR PSY-4QV3R1 showed the highest correlation with *in situ* measurements.

Keywords: Temperature, salinity, ice conditions, Polar Front, marginal ice zone, Kola Section, MERCATOR PSY4QV3R1, CMEMS GLORYS12v1, TOPAZ5, Barents Sea

© *Т. М. Максимовская*[1]*, *А. В. Зимин*[1], *О. А. Атаджанова*[1], *А. А. Коник*[1], *Е. С. Егорова*[2], *Д. В. Моисеев*[3], 2025
[1]Институт океанологии им. П.П. Ширшова РАН, 117997, г. Москва, Нахимовский проспект, д. 36
[2] Центр морских исследований МГУ им. М.В. Ломоносова, 119607, г. Москва, Раменский бульвар, д. 1, Кластер «Ломоносов», офис 1001
[3]Мурманский морской биологический институт РАН, 183032, г. Мурманск, ул. Владимирская, д. 17
*maximovskaja.t@yandex.ru

Изменчивость характеристик полярной фронтальной зоны в северо-западной части Баренцева моря по данным контактных наблюдений с 2017 по 2023 гг.

Статья поступила в редакцию 23.01.2025, после доработки 27.03.2025, принята в печать 10.06.2025

Аннотация

Приведены результаты океанографических наблюдений, выполненных с борта НИС «Дальние Зеленцы» на разрезе Кольский меридиан в 2017–2023 гг. Основной акцент сделан на оценках характеристик фронтальных разделов в области северной части Полярной фронтальной зоны Баренцева моря в осенний, зимний и весенний периоды. Для

Ссылка для цитирования: *Максимовская Т.М.*, *Зимин А.В.*, *Атаджанова О.А.*, *Коник А.А.*, *Егорова Е.С.*, *Моисеев Д.В.* Изменчивость характеристик полярной фронтальной зоны в северо-западной части Баренцева моря по данным контактных наблюдений с 2017 по 2023 гг. // Фундаментальная и прикладная гидрофизика. 2025. Т. 18, № 2. С. 41–57. https://doi.org/10.59887/2073-6673.2025.18(2)-3 EDN FSMDHC
For citation: Maksimovskaya T.M., Zimin A.V., Atadzhanova O.A., Konik A.A., Egorova E.S., Moiseev D.V. Variability of the Polar Front Characteristics in the Northwestern Barents Sea Based on In-Situ Observations from 2017 to 2023. *Fundamental and Applied Hydrophysics*. 2025;18(2):41–57. https://doi.org/10.59887/2073-6673.2025.18(2)-3

оценки аномалий ледовитости использовались данные Мирового центра данных по морскому льду (AARI WDC Sea-Ice). Выполнено сравнение результатов наблюдений в северной части разреза вблизи прикромочной ледовой зоны с характеристиками температуры и солености из глобальных океанологических баз. Для сравнения привлекались продукты MERCATOR PSY4QV3R1, CMEMS GLORYS12v1 и TOPAZ5. На всех разрезах были обнаружены высокоградиентные зоны, выраженные в поле температуры и солености, на разном расстоянии от кромки ледового поля. Было подтверждено, что в западном районе Баренцева моря отмечается устойчивый тренд к сокращению площади ледового покрова последние три десятилетия. Показано, что самый северный из фронтальных разделов Полярной фронтальной зоны Баренцева моря на оси разреза Кольский меридиан находился на расстоянии от 48 до 290 км от кромки ледовых полей, градиенты температуры варьировались от 0,10 до 0,20 °С/км, солености — от 0,012 до 0,025 епс/км, ширина фронтальной зоны не превышала 55 км. Наилучшее соответствие результатам измерений отмечено с данными продукта MERCATOR PSY4QV3R1.

Ключевые слова: температура, соленость, ледовые условия, Полярная фронтальная зона, прикромочная ледовая зона, Кольский меридиан, MERCATOR PSY4QV3R1, CMEMS GLORYS12v1 и TOPAZ5, Баренцево море

1. Introduction

The Barents Sea, largely situated on the continental shelf, is an interaction zone between Atlantic and Arctic waters (Fig. 1). The region's current system is determined by seabed topography [1, 2]. Atlantic waters enter the western part of the sea in two main flows [3]. The primary flow of warm (above 3 °C) and saline (above 34.8 psu) Atlantic waters primarily enters the Barents Sea through the Bear Island Trough with waters from the Nord Cape Current. The secondary flow consists of the Norwegian and Murmansk coastal currents, which transport waters with temperatures above 3 °C and salinities below 34.4 psu eastward. These flows toward the east are about 2 Sv [4] and 1.1 Sv [5], respectively.

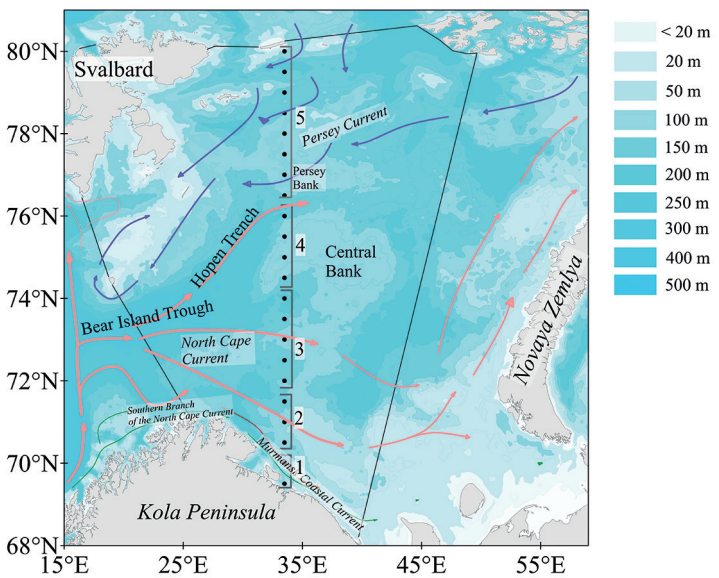

Fig. 1. Surface circulation in the western Barents Sea, with Atlantic waters (red arrows), Arctic waters of the Perseus Current (blue arrows), and the southern branch of the North Cape Current and Murmansk Coastal Current (green arrows) overlaid on a depth map from [3]. The Western region (WBS), Northeast (NEBS) and Southeast (SEBS) of the Barents Sea is highlighted by black lines. Dots indicate oceanographic station locations along the Kola Section. Numbers along the transect correspond to station groupings by current: 1 — stations in the Murmansk Coastal Current zone; 2 — Murmansk Current; 3 — Central branch of the North Cape Current; 4 — Northern branch of the North Cape Current; 5 — Perseus Current

Arctic waters enter the Barents Sea from the north and northeast, accompanied by drifting sea ice. These waters originate from ice melt and are characterized by negative temperatures and reduced salinity (below 34.7 psu). Estimating the volume and pathways of these waters remains a subject of debate [2, 6], due to challenges in conducting *in*

situ measurements in ice-covered regions. Direct current measurements from anchored stations are available at only two locations [2]. Estimates derived from geostrophic calculations range from 0.1 to 0.3 Sv, with model simulations suggesting a slightly higher value of 0.36 Sv [2]. In recent decades, the Arctic has undergone rapid warming, exceeding global averages [7]. This warming has led to significant reductions in sea ice extent and thickness, contributing to a decline in overall ice volume [8–10]. These changes influence the volume of Arctic waters entering the Barents Sea.

An important consequence of the interaction between Atlantic and Arctic waters in the Barents Sea is the presence of the North Polar Frontal Zone [10] or the more commonly used term Polar Front (PF) [11, 12]. This zone is characterized by strong horizontal and vertical gradients in temperature and salinity, spanning tens of kilometers. PF in the Barents Sea is considered quasi-stationary, with its position influenced by the slopes of major underwater elevations, including the Spitsbergen Bank, Central Bank, and Perseus Bank. It is typically found near the 200–250 m isobath [3, 12]. However, Ingvaldsen et al. [4] demonstrated that climate change is altering the front's position south of Bear Island, with warmer periods and stronger winds causing it to shift upward along the slope. In the Central Bank region, where the frontal zone is naturally less stable [3], these fluctuations may be even more pronounced.

Sea ice cover is both a key factor shaping the hydrological regime of the Barents Sea and an indicator of its variability [13]. Ice cover influences ocean–atmosphere interactions, regulating heat exchange and the mixing of water masses, particularly in the ocean's active layer. On average, the boundary of ice distribution in the Barents Sea lies north of the PF [14] and is referred to as the Marginal Ice Zone (MIZ). The MIZ represents a transition between open ocean and dense drifting ice, extending from the 15 % ice concentration arbitrary line to the 80 % ice concentration isoline [15]. A distinct haline frontal zone often forms near the MIZ during the warm season due to the inflow of meltwater, with its influence detectable several tens of kilometers from the ice edge [16].

In the context of climate change, there is a noticeable acceleration of warming rates in the Arctic, known as "Arctic amplification" [17–23]. Against this backdrop, the Barents Sea has seen the most significant decline in sea ice cover among Arctic seas [24], coupled with an overall increase in the average temperature of the air–ice–ocean system [18]. As a result, the Barents Sea becomes the first ice-free sea in the Arctic Ocean during the summer period. However, in the autumn, winter, and spring, ice formation still occurs in the northern part of the basin. As sea ice extent decreases, the intensity of interactions within the ocean–atmosphere system increases. Consequently, current climate conditions differ from those of previous years due to the increased air temperature across all seasons [2], inevitably affecting the position and characteristics of frontal zones in the sea. Since the early 21st century, the Barents Sea has undergone substantial changes, including a decline in sea ice extent, positive anomalies in sea surface and near-surface air temperatures, and rising temperatures in intermediate and deep waters [21, 25–27]. Between 1993 and 2018, the Barents Sea's annual heat balance remained negative across the entire basin, with winter heat flux increasing due to reduced ice cover and the inflow of warmer Atlantic-origin waters from the Norwegian Sea [28]. Studies indicate a significant negative linear trend in sea ice extent, mirroring changes across the broader Arctic region [29–31]. Over recent decades, the average annual ice cover of the Barents Sea has declined by 14.6 % per decade [23], underscoring the rapid transformation of the region's oceanographic conditions.

Hydrological fronts at the boundary between Atlantic and Arctic waters are a key oceanographic feature of the Barents Sea. However, their variability during the cold season has been insufficiently studied due to limited accessibility [16]. In recent years, research on these fronts has intensified [3, 11–12, 32–33]. This study contributes to the understanding of the northern part of the Polar Front (PF) through recurring observations along the Kola Section, a long-term monitoring transect at 33°30′ E [34]. Observations have been conducted at this site for over a century, with the first studies taking place in May 1900. Throughout the past century, numerous investigations have been carried out [1, 35–40]. Observations along this transect provide valuable data for monitoring seasonal and interannual variations in oceanographic parameters, particularly along the path of Atlantic-origin waters, which influence the characteristics of the Polar Front. However, research on this transect north of 74°N was not typically conducted during the ice formation period. It is only in recent decades, coinciding with the active decline of sea ice extent in the Barents Sea, that the Murmansk Marine Biological Institute of the Russian Academy of Sciences (MMBI RAS) has regularly conducted studies along the transect up to the MIZ [41].

Studies along the Kola Section aim to continuously monitor the marine environment, enhancing the quality of forecasts for anticipated changes. Currently, addressing this task involves developing numerical models that incorporate operational assimilation of satellite, drifter, and ship-based observational data. Global ocean reanalysis systems are continually evolving, with their outputs being publicly accessible (e. g., Copernicus Marine Environment Monitoring Service, Arctic Ocean Physics Analysis and Forecast). The generated spatio-temporal fields of oceanographic characteristics are regularly updated and allow for the reproduction of oceanic fields of temperature and salinity, which are considered verified. However, regular data from Arctic seas are only available from certain satellite observational systems and coastal stations. Irregular data obtained from localized marine expeditions often fail to enter

assimilation models due to fragmentation and strict internal regulations within marine organizations and research institutes. Independent verification of the products is rarely conducted, especially involving databases that were not part of the development process of the analyzed models. The availability of a unique dataset enables the assessment of how accurately oceanographic fields are reproduced by different reanalysis types.

The aim of the study is to assess the variability of the PF characteristics in the northwestern Barents Sea based on *in situ* observations along a regularly conducted hydrological transect, while accounting for changes in sea ice extent. Additionally, the study aims to evaluate the quality of oceanographic field reproduction using various reanalysis and forecasting products.

2. Materials and Methods

This study uses expedition data collected by the MMBI RAS in the western Barents Sea [42–43] on board the research vessel (R/V) "Dalnie Zelentsy" from 2017 to 2023. Oceanographic research was conducted along the Kola Section (Fig. 1). Key hydrological parameters of the marine environment were measured using CTD (Conductivity, Temperature, Depth) casts with a SEACAT SBE19 Plus V2 profiler. This work includes a series of oceanographic measurements taken from 69°30' N along the 33°30′ E meridian to the ice edge, with a spacing of 15–30 nautical miles across different seasons from 2017 to 2023 (Table 1). Due to the technical specifications of the research vessel, measurements were conducted in conditions of low ice consolidation (1–3 points on the ice scale).

Table 1

Description of *in situ* data

Research Dates	Number of Stations Completed	The position of the ice edge on the axis of the Kola section., N
13–17 July 2017 г.	28	78°35′
29 November — 4 December 2017 г.	35	79°21′
14–16 May 2018 г.	34	77°57′
12–14 March 2022 г	30	77°09′
4–8 January 2023	33	77°55′
24–27 April 2023	25	75°21′
8–15 May 2023	23	75°49′
20–26 November 2023	33	77°45′

For the verification and supplementation of visual observations of the ice edge conducted from the R/V, data from the U.S. National Ice Center[1] archive were used. These data represent a shapefile containing vector information on the location of the MIZ, where sea ice concentration is less than 80 %, and the pack ice zone, where the ice concentration is greater than 80 % (Fig. 2).

The main source of ice information was the Arctic and Antarctic Research Institute (AARI) ice charts, compiled by ice experts with many years of experience. The archive of ice charts is collected in the electronic catalog of the World Data Center for Marine Ice[2]. In the construction of ice charts, satellite images in various electromagnetic spectrum ranges (visible, infrared, and microwave) are used to obtain the necessary information about the ice cover, supplemented by data from ship-based observations and polar hydrometeorological stations. The AARI ice charts are available with a weekly frequency, starting from October 1997 to the present. A detailed description of the methodology for compiling AARI ice charts is presented in the paper by Afanasyeva [44]. As a result, ice cover was calculated as a percentage of the extent of the western region, which is one of the homogeneous ice hydrological zones of the Barents Sea, within the commonly accepted boundaries. The lower limit for the determination of ice concentration is 10 %, corresponding to 1 point on the ice chart.

The classification of monthly ice conditions anomalies was performed according to the methodology in [45]. The average monthly ice anomalies (ΔS_ice) were compared with the given values of the standard deviation of ice concentration from the 27-year average, σ. The average monthly ice anomalies, calculated for the western region of the Barents Sea, were classified into five categories (Table 2). The criteria for classifying anomalies were based on the objective property that the repeatability of anomalies is inversely proportional to their magnitude [46].

[1] U.S. National Ice Center: [website]; URL: https://usicecenter.gov/Products/ArcticHome (accessed on 20.09.2024)
[2] AARI WDC Sea_Ice: [website]. URL: http://wdc.aari.ru/datasets/d0015/ (accessed on 28.09.2024)

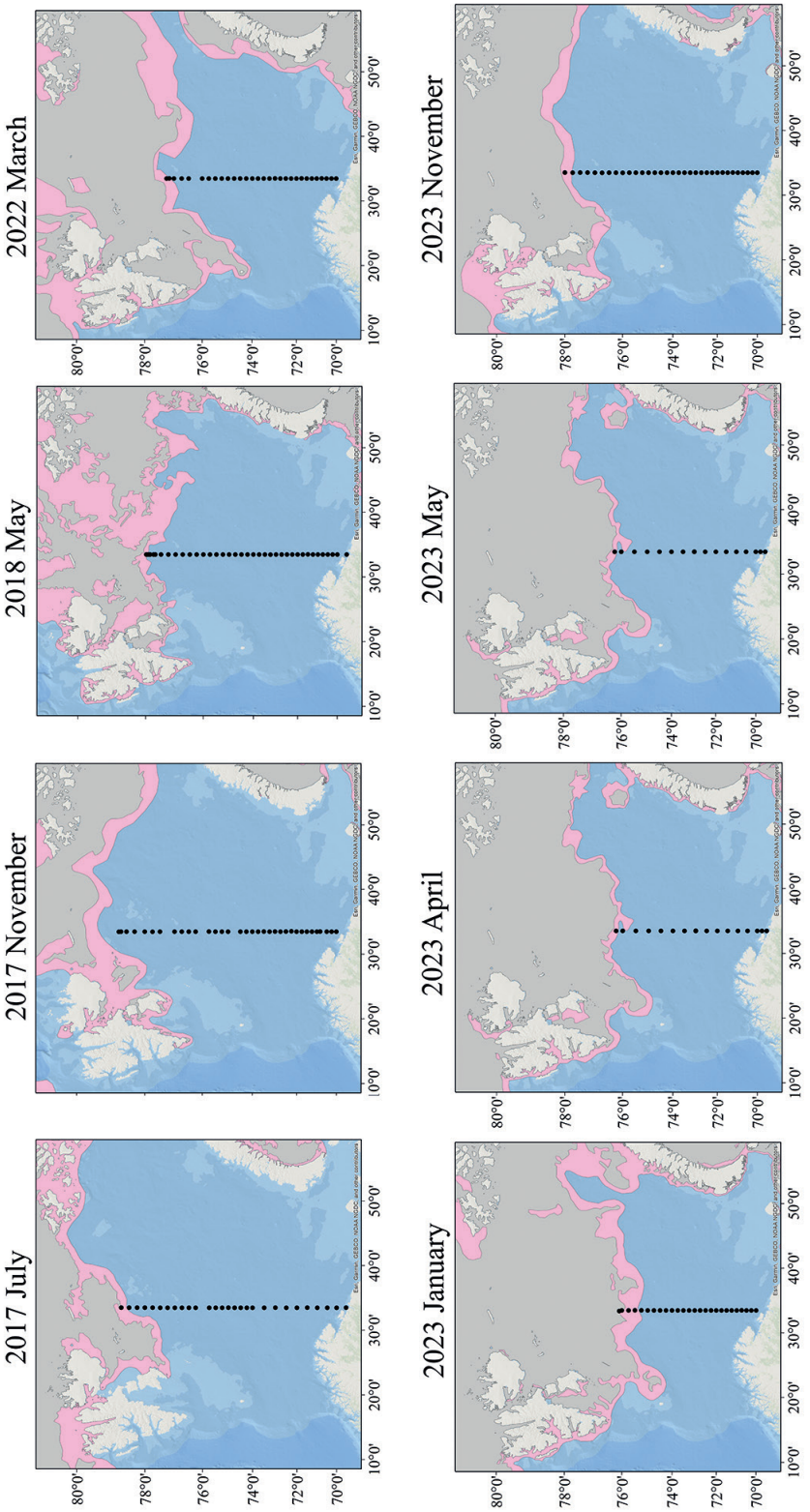

Fig. 2. Location of the oceanographic stations along the Kola Section on the map of the Barents Sea. The position of the MIZ is highlighted in pink (1–8/10 concentration), and areas of consolidated ice (> 8/10 concentration) are shown in gray

The criterion for evaluating the thermal state of the waters in the Barents Sea was the ratio of water temperature anomalies (ΔT) in the 0–50 m layer at standard stations along the Kola Section profile (69°30′ — 74° N, with a 30′ interval) for each period (month) when contact measurements were made, and the standard deviation of water temperature (σ) categorized into five gradations [47–48] (Table 2). The classification of water temperature anomalies was carried out according to two sets of climatic norms. In the first case for calculating the anomalies, monthly water temperature norms were used, derived from data from 1970 to 2019 from the World Ocean Database[3], ICES[4], and local databases from the MMBI RAS. The norms and anomalies were calculated with a five-meter depth interval. In the second case, the data on the climatic average temperatures of the water was obtained from the World Ocean Atlas[5]. The atlas shows the statistical average value of the water temperature in the grid nodes with a resolution of ¼ degree for the climatic period from 1991 to 2020 for each month.

Table 2

Gradations of sea ice anomalies in the western Barents Sea region and temperature anomalies along the Kola Section in the 0–50 m layer

Type of anomaly	Gradations of Sea Ice Anomalies, the fraction of σ	Gradations of Temperature Anomalies, the fraction of σ
Very strong positive anomaly (+VSA)	$\Delta S\_ice > 1.2\sigma$	$\Delta T > 1.5\ \sigma$
Strong positive anomaly (+SA)	$0.4\sigma < \Delta S\_ice \leq 1.2\sigma$	$0.5\ \sigma < \Delta T \leq 1.5\ \sigma$
Close to norm (N)	$\pm\ \Delta S\_ice \leq 0.4\sigma$	$\pm\ \Delta T \leq 1.5\ \sigma$
Strong negative anomaly (–SA)	$0.4\sigma < -\Delta S\_ice \leq 1.2\sigma$	$0.5\ \sigma < -\ \Delta T \leq 1.5\ \sigma$
Very strong negative anomaly (–VSA)	$-\Delta S\_ice > 1.2\sigma$	$-\Delta T > 1.5\ \sigma$

The frontal zone is a zone within which spatial gradients of temperature and salinity (∇T and ∇S) are significantly sharper compared to climatological values [49]. Therefore, the gradients in the frontal zone must substantially exceed the average climatological gradient (∇Climat(T/S)). In the study [49], it is proposed to identify frontal zones when the gradients of T/S exceed 10 climatic gradients of the corresponding characteristics. Climatological values for the horizontal temperature and salinity gradients for the Barents Sea, according to [10], do not exceed 0.01 °C/km and 0.001 psu/km, respectively. The width of the frontal zone was determined as the distance between points (stations) along the profile, beyond which the temperature and salinity gradients approach climatological values. Isotherm 1.5 °C and isohaline 34.7 psu, characteristic of the position of the main frontal boundary (the line corresponding to the maximum gradient values within the frontal zone), were selected between such stations.

To assess the impact of wind forcing on the dynamics of the ice edge position, the U and V components of the hourly wind speeds at 10 m height from the ERA5[6] reanalysis were used. The wind speed and direction in knots were calculated at the grid points corresponding to the first point north of the ice edge position along the meridian 33°30' E. Additionally, air temperature at 2 m height was taken from the reanalysis, averaging over the segment of the profile from the position of the frontal zone to the ice edge. The period considered was four days: three days prior to the ice edge measurements and the day of the measurements.

To compare the results of CTD profiling with operational ocean model data, daily data from the following products were used:

– MERCATOR PSY4QV3R1[7];
– TOPAZ5[8];
– CMEMS GLORYS12v1[9].

[3] NOAA World Ocean Database: [website]. URL: https://www.ncei.noaa.gov/products/world-ocean-database (Accessed: 1.09.2024)
[4] ICES: [website]. URL: https://www.ices.dk/data/data-portals/Pages/ocean.aspx (Accessed: 1.09.2024)
[5] World Ocean Atlas: [website]. URL: https://www.ncei.noaa.gov/access/world-ocean-atlas-2023/bin/woa23.pl (Accessed: 02/25/2025)
[6] ECMWF: [website]. URL: https://cds.climate.copernicus.eu/datasets (Accessed: 1.11.2024)
[7] Global ocean 1/12° physics analysis and forecast updated daily: [website]. URL: https://data.marine.copernicus.eu/product/GLOBAL_ANALYSISFORECAST_PHY_001_024 (Accessed: 05.09.2024)
[8] Arctic Ocean Physics Analysis and Forecast: [website]. URL: https://data.marine.copernicus.eu/product/ARCTIC_ANALYSISFORECAST_PHY_002_001 (Accessed: 05.09.2024)
[9] Global ocean physics reanalysis: [website]. URL: https://data.marine.copernicus.eu/product/GLOBAL_MULTIYEAR_PHY_001_030 (Accessed: 05.09.2024)

The selection of the CMEMS GLORYS12v1, MERCATOR PSY4QV3R1, and TOPAZ5 products was based on their high spatial and temporal resolution for the study region. The CMEMS GLORYS12v1 product from the Copernicus Marine Environment Monitoring Service is a global ocean reanalysis with daily resolution and a spatial resolution of 1/12°. The MERCATOR PSY4QV3R1 product, the operational global ocean analysis and forecasting system of the European group, has the same resolution. The TOPAZ5 daily data set, which uses the HYCOM model, provides information for the Arctic region with a spatial resolution of 6.25 km for the output data.

The region from 74° to 80° N and 33° to 34° E was extracted from the products, containing data on the distribution of temperature and salinity in the 0–50 m layer across 19 depth levels corresponding to the grid nodes of the CMEMS GLORYS12v1 and MERCATOR PSY4QV3R1 products, and 11 depth levels for the TOPAZ5 product. For the comparative analysis, uniform arrays were formed by aligning measurement data and model products to common coordinates, depth levels, and dates of each station along the transect. All data along the transect were interpolated using the Kriging method [50], which provides the best linear unbiased estimate of field characteristics on a regular grid, in Surfer software. The comparative analysis included both qualitative and quantitative assessments of how well the reanalysis and forecast data corresponded to the in-situ measurements.

For the comparative analysis, the Modified Hausdorff Distance (MHD) was used. This metric is often employed for quantitatively assessing the similarity between the spatial distribution of modeled and observed scalar fields of various hydrometeorological parameters [51, 52]. In the frontal zone, the isotherm of 1.5 °C and the isohaline of 34.7 psu, corresponding to the center of the frontal zone based on in-situ data, were selected. For the selected products, the same isotherms (temperature) and isohalines (salinity) were chosen. Each point on the isotherm had its own coordinates, with the x-axis representing the distance along the transect in kilometers and the y-axis representing the depth. As a result, Set A formed a set of points (with coordinates along the x and y axes) based on in-situ observations, and Set B formed a set of points from one of the products. Further explanations are given in terms of set theory. For the comparison, the characteristic isotherm of 1.5 °C and isohaline of 34.7 psu, typical for the position of the maximum gradient in the frontal zone, were selected.

Initially, the minimum distance from the set of points A to each point b was calculated (1), followed by a similar calculation from each point a to the set of points B (2).

$$d(A,b) = \inf_{a \in A} d(a,b), \tag{1}$$

$$d(a,B) = \inf_{b \in B} d(a,b). \tag{2}$$

Next, the average minimum distances within the sets are calculated (3).

$$d(A,B) = \frac{1}{|A|} \sum_{a \in A} d(a,B), \tag{3}$$

where $|A|$ and $|B|$ are the number of points in each set, respectively. At the final stage, the maximum value is selected from the available average minimum distances between the sets of isoline points (4) for each horizon.

$$MHD = \max\{d(A,B), d(B,A)\}. \tag{4}$$

For a qualitative assessment in the frontal zone between two stations where the FZ was located, the gradient at each depth was calculated based on the data (in the case of *in situ* data interpolated to depths for CMEMS GLORYS/MERCATOR PSY4QV3R1 and TOPAZ5). The weighted average gradient was then computed. The gradient anomaly (An. Grad), or the difference between the weighted average gradient based on *in situ* data and the weighted average gradient of the product was assessed. The significance of the difference was evaluated using Fisher's criterion [53], which was compared with the critical value. If the calculated value was greater/less than the critical value, the differences between the weighted averages were considered significant or insignificant, respectively.

For a qualitative assessment in the frontal zone area between two stations where the FZ was located, the gradient was calculated at each depth level based on the data (in the case of *in situ* data, interpolated to the depths for CMEMS GLORYS/MERCATOR PSY4QV3R1 and TOPAZ5). The weighted average gradient was then computed. Next, the difference between the weighted average gradient from *in situ* data and the weighted average gradient from the product was evaluated. The significance of differences between the means was assessed using Student's t-test [53], which was compared with the critical value at a significance level of $\alpha = 0.05$. If it was greater or smaller, the differences between the weighted average values were considered significant or not significant, respectively.

3. Results

3.1. Changes in ice cover in the western Barents Sea

According to the annual average data, the ice cover in the western Barents Sea has been decreasing over the past 30 years (Fig. 3). Maximum ice coverage during the observed period occurred in 2003, while minimum coverage was recorded in 2016. Since 2018, a steady decline in the ice-covered extent has been observed. Over the past decade, the ice extent has decreased by 4.4 %, which is approximately three times smaller than the decline observed across the entire sea [23]. In addition to the pronounced negative trend in ice coverage in the western region, interannual variability also includes cyclic components with periods ranging from 4 to 11 years, which significantly contribute to the variability of the series.

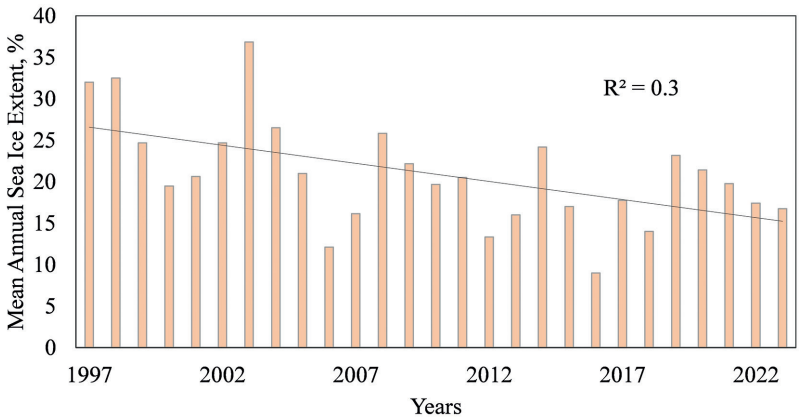

Fig. 3. Mean annual sea ice extent in the western Barents Sea from 1997 to 2023

Monthly anomalies of ice coverage in the studied region for the periods of work along the Kola Section are shown in Table 3. These anomalies indicate the absence of positive sea ice anomalies during all months of the expeditionary studies. The types of water temperature and sea ice anomalies are well correlated (Table 3). Accordingly, positive water temperature anomalies were associated with negative sea ice anomalies in the western Barents Sea. A negative anomaly was observed twice in May, suggesting an earlier onset of the ice melting process in recent years. The water temperature anomaly in the 0–50 m layer along the Kola Section exhibited normal and positive values.

The presented results also confirm that the variability of the sea ice regime in the Barents Sea is not homogeneous, with most of this variability occurring in the central and northeastern parts of the sea [54]. The significant influence of the inflow of Atlantic-origin waters on maintaining the ice-free conditions in the southwestern Barents Sea has been demonstrated in previous studies [55, 56].

Table 3

Classification by type of anomaly

Measurement period	Type of average monthly ice coverage anomaly	Temperature anomaly types (norms from 1990 to 2020)
2017 July	N	–SA
2017 November	–SA	N
2018 May	–SA	+SA
2022 March	N	+SA
2023 January	–SA	+VSA
2023 April	N	+SA
2023 May	–SA	N
2023 November	N	N

Note: Very strong positive anomaly (+VSA), Strong positive anomaly (+SA), Close to norm (N), Strong negative anomaly (–SA).

During the months analyzed in the last decade, predominantly anomalously warm years and warm conditions in terms of water temperature were observed, corresponding to significant negative and normal ice coverage

anomalies in the western Barents Sea. This reflects the ongoing trend of significant ice cover decline in the Barents Sea over recent decades. The effects of these changes on the characteristics of the PF will be considered in the following section.

3.2. Characteristics of Water along the Kola Section during the Summer Season

The only summer measurements along the Kola Section in the considered set of contact observations were conducted in July 2017. This period (July 2017) was characterized by a strong negative temperature anomaly in the 0–50 m layer and an ice cover in the western area of the Barents Sea that was close to normal (Table 3). The ice melting season in the Barents Sea begins in May and lasts until September, during which the ice edge retreats northward and eastward [2]. Stations along the Kola Section can be grouped into five categories based on the currents crossing the section (Fig. 1, 5). The positions of boundaries between station groups may vary depending on climatic conditions and the impact of synoptic-scale processes.

The first group of stations is located in the waters of the Murmansk Coastal Current (69°30′–70°00′ N). Here, the freshwater influence from river runoff is observed, resulting in a distinct halocline throughout the year. In July 2017, this halocline was observed in the 0–10 m layer, with a salinity gradient of 1.6 psu/km and a temperature gradient of 4.9 °C/km. The average temperature and salinity at the stations were 5 °C and 34.4 psu.

The second group of stations is crossed by the Murmansk Current (70°30′–71°30′ N). In this section of the transect, the Murmansk Coastal Current interacts with the Murmansk Current. The influence of river runoff gradually decreases toward the north, and the halocline rises to the surface. The average temperature and salinity in this zone in July 2017 were 5 °C and 34.7 psu. At the northern boundary of this station group, the Coastal Front Zone is observed, manifested in the salinity field.

The third group of stations belongs to the Central Branch of the North Cape Current (72°00′–74°00′ N). This group of stations has the most homogeneous structure during the winter period, both in terms of temperature and salinity. In summer, a warm upper layer and colder bottom waters are observed. The average temperature and salinity values were 4.1 °C and 35 psu, respectively.

The fourth group is in the region influenced by the Northern Branch of the North Cape Current and the Central Current (74°15′–76°15′ N). The upper 50-meter layer is occupied by warm Atlantic waters, with average temperature and salinity values of 4.2 °C and 34.9 psu. Below the Atlantic waters, a dome of cold, salty Barents Sea waters is observed, with average temperature and salinity values of 2 °C and 35 psu. The northern part of this region contains the Polar Front of the Barents Sea.

The fifth group of stations is located in the region influenced by the Perseus Current (76°30′–80°00′ N). Here, cold Arctic waters with temperatures below 0 °C are observed. Freshened waters, formed as a result of mixing local waters with meltwaters, occupy a layer from the surface to 100 meters. The average temperature and salinity in this layer were –0.1 °C (excluding the warmed upper 20-meter layer) and 34.5 psu. The minimum temperature was –1.8 °C. The most freshened layer, from the surface to 15 meters, characteristic of the active ice-melting period, was observed in the northern part of the section, with the minimum salinity of this layer being 32.2 psu.

At the boundary between the fourth and fifth groups of stations, there is the Polar Front of the Barents Sea, located in the region of the Perseus Current slope. This frontal zone is often situated close to the ice edge or is entirely covered by ice of varying cohesion during the winter period. The existence of the frontal zone is due to the interaction between the Arctic waters of the Perseus Current and the Atlantic waters of the Northern Branch of the North Cape Current. Since the Polar Front is a zone where cold, fresh waters from the Arctic Basin interact with warm, salty Atlantic waters, it is expressed both in the temperature field and the salinity field. The zones of sharp gradients in temperature and salinity do not always coincide, and in the salinity field, a double (stepped) structure is observed. This frontal zone has a quasi-stationary nature and exists throughout the year.

Measurements in the Polar Front zone were taken from July 15 to 17, 2017. During this time, the average air temperature at a height of 2 meters (according to Era5 data) was 3.14 °C, with a prevailing southward wind at a speed of 5.2 m/s. The ice edge was observed at 78°35′ N. The upper 20–25-meter layer was warmed to 2 °C. The zone of maximum vertical temperature gradients extended under the warmed waters up to 150 meters. The width of the frontal zone was about 55 km, with a temperature gradient of 3.1 °C/km at a 30-meter depth. North of 78°30′ N, Arctic waters had a negative temperature from the surface to the bottom and were within the Polar Front. The maximum horizontal temperature gradient exceeded the climatic one by 12 times, and the salinity gradient exceeded the climatic one by 14 times. Two regions of increased salinity gradients were distinguished along the section. The first region was observed near the slope of the Perseus Bank, where the Polar Front is located. The second region of increased gradient was found 65 km from the ice edge, where it was more pronounced in the salinity distribution.

Here, 0–10-meter layer of the most freshened and coldest waters, formed directly by ice melt in the study region, was observed, with the minimum salinity of 32.1 psu. It is also worth noting that this distribution [10] is called "stepped", distinguishing types of internal structure in frontal zones along with "interspersed" ones. In this section of the Polar Front, such a "stepped" type is characteristic only in the summer season in the salinity distribution when active ice melting occurs. Thus, the first zone corresponds to the Polar Front of the Barents Sea, while the second freshened zone corresponds to the Arctic Frontal Zone [10], whose formation is associated with ice melting in the warm period of the year. This last frontal zone is often noted in the PF zone, as it was in this case (Fig. 4a).

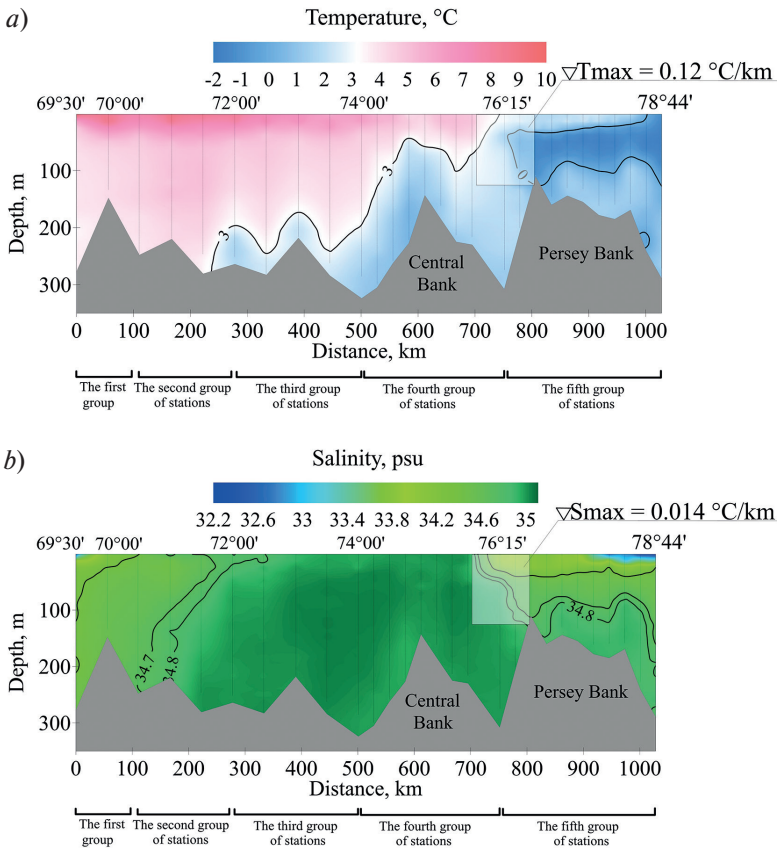

Fig. 4. Vertical distribution of temperature (*a*) and salinity (*b*) along the Kola Section close to normal background conditions in the summer of 2017. The positions of the Polar Front are highlighted with rectangular zones, and the maximum temperature gradient (∇Tmax) and salinity gradient (∇Smax) are indicated

3.3. Characteristics of Waters along the Kola Section during the ice formation period

The remaining measurements were primarily taken during the winter season (Table 4), which marks the beginning of the sea ice formation period in the Barents Sea. The sea ice formation period in the Barents Sea typically begins in early October in the northern regions and lasts until March-April, when the ice cover reaches its maximum extent [2]. The studies conducted in November 2017, January 2023, and November 2023 coincide with the onset of the ice formation period. During this time, the waters are relatively homogeneous, unaffected by radiation heating and additional freshening due to ice melt.

At the end of November 2017 and January 2023, measurements were taken under conditions of a very large positive anomaly and normal in water temperature in the 0–50 m layer and a large negative anomaly in ice cover in the western Barents Sea. As a result, the waters were warmer than usual, and the extent covered by ice was smaller than in 'close to normal' conditions. In the 'close to normal' ice cover and water temperature conditions for the western Barents Sea, measurements were taken in November 2023. During the periods of measurement, air temperatures were below zero, the prevailing wind direction varied from year to year, and the average wind speed did not exceed 6.3 m/s. The southern boundary of the thermal frontal zone varied from 76°15' N in November 2017 and January

2023 to 76°30′ N in November 2023. The width of the frontal zone was about 30 km, and vertically, the boundary of the thermal frontal zone extended from the surface to 100–150 m. Since, at the beginning of the winter period, the ice cover forms from the northern part of the sea towards the south, the frontal zone was located at a considerable distance from the ice edge. For example, in November 2017, the thermal and haline frontal zones were almost 300 km from the ice edge. The maximum horizontal temperature gradient at the beginning of the ice formation period exceeded the climatic norm by 10 to 16 times, and the maximum salinity gradient was 13 to 25 times greater than normal.

Table 4

Position and characteristics of the Polar Front along the Kola Section

Measurement period	The position of the thermal frontal zone, N	Maximum temperature gradient, °C/km	Position of the salinity frontal zone, N	Maximum salinity gradient, psu/km
2017 July	76°00′–76°30′	0.12	75°45′–76°00′	0.014
2017 November	76°30′–76°45′	0.11	75°15′–76°45′	0.025
2018 May	76°00′–76°30′	0.12	76°00′–76°30′	0.021
2022 March	76°00′–76°30′	0.12	76°00′–76°30′	0.025
2023 January	76°15′–76°30′	0.16	76°15′–76°45′	0.020
2023 April	75°30′–75°45′	0.10	75°30′–76°00′	0.012
2023 May	76°00′–76°15′	0.20	76°00′–76°15′	0.018
2023 November	76°30′–76°45′	0.10	76°30′–76°45′	0.013

At the end of the ice formation season, when the ice cover in the Barents Sea reaches its maximum extent, measurements were taken in May 2018, March 2022, April, and May 2023. All measurements during this period were taken under conditions of a strong positive anomaly (May 2018, March 2022, April 2023) and close to normal (May 2023) in temperature along the section, and normal (March 2022 and April 2023) and strong negative anomaly (May 2018 and 2023) in ice cover in the western Barents Sea. The prevailing wind in March 2022 and April 2023 was from the north, with average speeds of 11.7 and 10.7 m/s, while in May 2018, the prevailing wind was from the east (4.6 m/s), and in May 2023, from the south (4.8 m/s). During the study period, the thermal and haline frontal zones coincided along the section. Compared to the start of the winter period, the frontal zone shifted south by 110 km in April 2023 and by 55 km in the other periods. The width of the frontal zone ranged from 30 to 55 km. The frontal zone was closest to the ice edge in April 2023. During the measurement period, three northern stations along the section were within the marginal ice zone. The frontal zone shifted south to 75°30′ N. The southward shift of the frontal zone was likely caused by the impact of the northern wind, which had a relatively high average speed (10.7 m/s). Two weeks later, measurements were taken again along the section. The frontal zone had shifted north to 76°00′ N, with the prevailing southern wind pushing the ice and Arctic waters to the north.

The classification of sea ice anomalies in the western Barents Sea, combined with the classification of water temperature anomalies in the 0–50 m layer along the Kola Section, revealed that in the last decade, negative sea ice anomalies have been predominantly observed alongside increased water temperature anomalies. Notably, the thermal component of the PF remained relatively stationary in years with varying climatic conditions (in November, at 76°30′–76°45′ N), with maximum horizontal temperature gradient values of 0.11 and 0.10 °C/km. The haline component, however, shifted 27 km southward along the Persey Bank slope (75°15′ N) in November 2017, when a large negative sea ice anomaly coincided with a close-to-normal water temperature, compared to its position in the climatically normal November of 2023. The maximum salinity gradient also differed significantly between these two measurement periods: in November 2017, it was twice as large as the corresponding value in November 2023. In May 2018 and 2023, similar background conditions were observed: strong negative sea ice anomalies alongside normal and strong positive water temperature anomalies. During these periods, the PF remained in stable coordinates along the transect (76°00′–76°30′ N). The dynamics of the frontal zone's position within the annual variability were also observed, with the frontal zone moving along with the ice edge position, predominantly during the winter months. However, the study focused on the highly dynamic upper 50-meter layer, which is significantly influenced by atmospheric and ice processes. In the study by [11], the intermediate water layer (50–130 m) in the Polar Front at the periphery of the Hopen Basin and Olga Basin, which is also considered highly dynamic, was examined. It was shown that a characteristic isotherm shifted nearly 25 km over 3–4 days. The authors attribute such short-term variability to tidal currents and mesoscale eddies. Thus, it can be suggested that the combined influence of atmospheric, ice, tidal, and eddy processes contributes to the shift in the position of the Polar Front under changing climatic conditions.

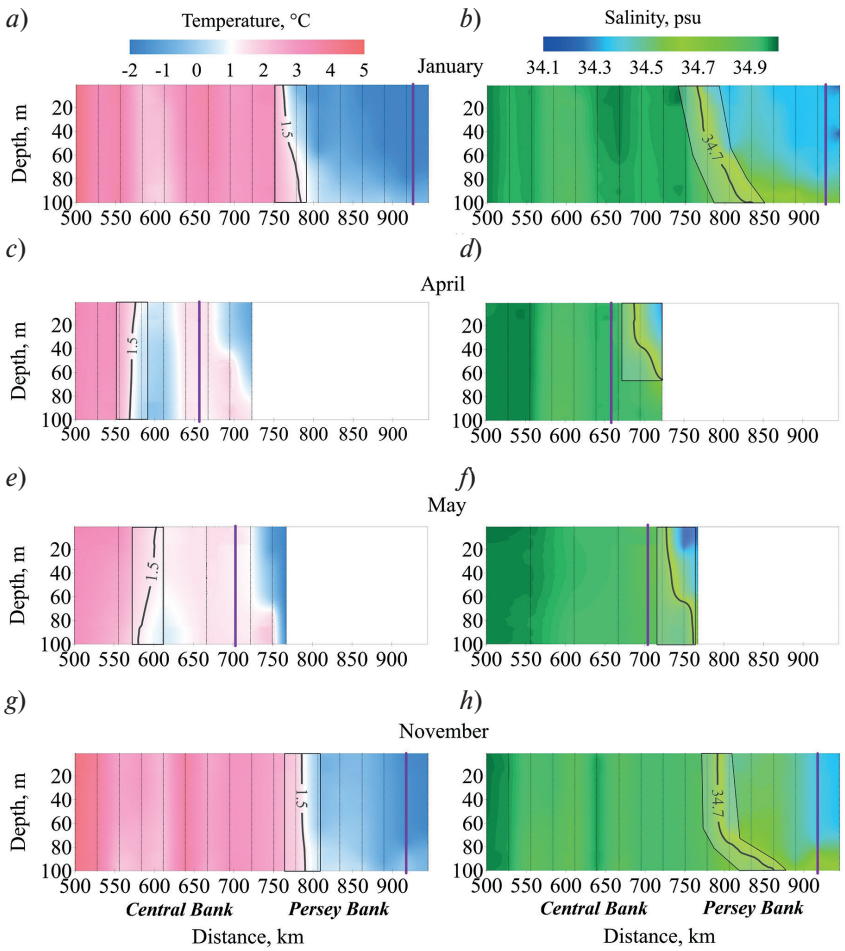

Fig. 5. Vertical distribution of temperature and salinity in the northern part of the Kola Section in 2023. The ice edge position is marked with a purple line. The zones of the thermal and haline components of the Polar Front are marked by polygons on the transect charts

The boundary of the thermal frontal zone shifts southward during the spring months. Thus, at the beginning of the ice formation period (January and November, Fig. 5ab, gh), the thermal component of the Polar Front was located above the slope of the Persey Bank, while at the end of this period (April, May, Fig. 5cd, ef), it was observed above the Central Bank. The frontal zone was closest to the ice edge (48–72 km) at the end of the ice formation period (April and May 2023), which was associated with the southward displacement of Arctic waters along with the ice cover. The haline frontal zone exhibited greater variability than the thermal one. At the end of the ice formation period, a more complex temperature distribution structure was observed in the PF compared to the earlier months of the season. An "alternating" temperature distribution was seen, characterized by the alternation of cold and warm patches of varying widths, separated by local fronts. The formation of such a structure could have been caused by both advection processes and the influence of vortices, which frequently form in the frontal zone [10]. For a more detailed study of the dynamics of the position and characteristics of the Polar Front, regular data is required, which cannot be obtained solely through expeditionary research. Therefore, it is essential to involve additional data that can be provided by various reanalysis models. To do this, having a set of field data allows us to compare it with model data and identify the most suitable one for the area under consideration.

3.4. Assessment of the reproducibility of water characteristics in the northwestern Barents Sea

To assess the quality of the reproduction of thermohaline fields in the PF of the Barents Sea along the Kola Section, a comparison was made between CTD profiling data and simulation results. Three measurement datasets were considered, collected during the sea ice formation period (January and November 2023) and during the transition from ice formation to ice melt (April 2023). The characteristic isolines for maximum temperature and salinity gradi-

ents (1.5 °C and 34.7 psu) were compared between *in situ* data and reanalysis data. In general, for all the considered months, the isotherm was located almost perpendicularly downward (Fig. 6a-c). The *in situ* isotherm was closest to the CMEMS GLORYS12v1 in April (1.1 km) and the MERCATOR PSY4QV3R1 in January (2.6 km). In other cases, the isotherms were located more than 3 km apart according to the MHD. The best result (minimal distance) for the 34.7 psu isohaline was shown by TOPAZ5 in January, with an MHD value of 5.3 km. However, in November of the same year, this value was nearly 14 times greater. The isolines for all products did not completely match with the *in situ* isolines, which is confirmed by the values presented in Table 5.

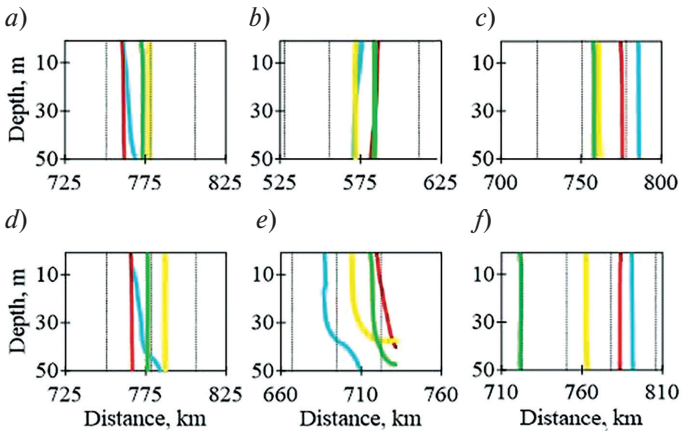

Fig. 6. Position of the 1.5 °C temperature isolines (a-c) and 34.7 psu salinity isolines (d-f) along the sections for January 7–8 (a, d), April 27 (b, e), and November 26 (c, f). Dashed lines represent the positions of oceanographic stations, with blue for in situ, red for MERCATOR PSY4QV3R1, green for TOPAZ5, and yellow for CMEMS GLORYS12v1

Table 5 also presents the values of the difference between the area-weighted gradients within the frontal zone based on *in situ* data and the data from the MERCATOR PSY4QV3R1, CMEMS GLORYS12v1, and TOPAZ5 products. The differences in the average area-weighted values of temperature and salinity gradients were assessed using Fisher's criterion (significance level $\alpha = 0.05$). Overall, the average values from *in situ* data and reanalysis products were not significant, except for the CMEMS GLORYS12v1 product regarding temperature and salinity in November 2023 and for MERCATOR PSY4QV3R1 concerning salinity in April 2023, when the difference between the area-weighted values was negligible, amounting to almost 0 °C/km. While the qualitatively selected reanalysis products do not precisely represent the real gradient values within the frontal zone, their positioning was sufficiently accurate for assessing the dynamics of the frontal zone's location across various temporal and spatial scales. When comparing the results of the reanalysis integrated over the three considered months, the MERCATOR PSY4QV3R product stood out as best representing the real conditions. The maximum MHD metric for the 1.5 °C isotherm reached values of up to 10.3 km, while for the isohaline, it was 26.2 km, with the maximum distance between the isolines observed reaching 69.2 km in conjunction with TOPAZ5 data.

Table 5

Values of the MHD between the positions of the isolines from *in situ* data and selected products, as well as the differences between the weighted averages of gradients within the frontal zone based on *in situ* data and selected products

Sources of the data sets being compared	January		April		November	
	MHD, km	An. Grad, °C(psu)/km	MHD, km	An. Grad, °C(psu)/km	MHD, km	An. Grad, °C(psu)/km
Temperature						
In situ — MERCATOR	2.6	0.0450	8.6	0.037	10.3	0.028
In situ — TOPAZ5	7.8	0.0720	10.9	0.062	27.8	0.061
In situ — GLORYS12v1	12.6	0.071	1.1	0.026	24.6	0.072
Salinity						
In situ — MERCATOR	5.9	–0.0003	26.2	0.0027	7.5	0.0008
In situ — TOPAZ5	5.3	0.0063	22.1	–0.0007	69.2	0.0080
In situ — GLORYS12v1	14.7	0.0075	11.7	0.0005	28.4	0.0101

The analysis of qualitative and quantitative evaluations from the comparative analysis showed that reanalysis and forecast products do not accurately reproduce the actual values of temperature and salinity within the frontal zone. However, the reanalysis data do not ensure the precise determination of temperature and salinity values in the Barents Sea. At the same time, they adequately describe the patterns of distribution of the studied parameters. This study demonstrated that the global product MERCATOR PSY4QV3R1 provided the most accurate values for the gradient and the position of isolines characteristic of the frontal boundary during the freezing period (January and November 2023). In the transitional period, when the sea experiences maximum coverage in the annual cycle and the melting process begins (April 2023), the variability of temperature and salinity in the Polar Front was well reproduced by the regional reanalysis product TOPAZ5.

4. Conclusions

The study presents the results of oceanographic observations conducted from the R/V "Dalnie Zelentsy", primarily in the northern part of the Kola Section during different seasons from 2017 to 2023. The position and characteristics of the Polar Front in the Barents Sea along the Kola Section are discussed for periods of active ice formation, maximum ice cover, transition to ice melting, and summer, when the ice edge reaches its northernmost position. The study focuses primarily on the highly dynamic upper 0–50 m water layer, which is more susceptible to variability due to ocean-ice-atmosphere interactions.

It has been confirmed that the ice extent in both the western Barents Sea and the entire basin has been gradually decreasing over the past decades. Over the last ten years, the ice area has shrunk by 4.4 %, which is more than three times less than the overall reduction across the entire Barents Sea. The analysis of sea ice anomalies revealed no positive anomalies during the months of observations. Negative anomalies in May could indicate an earlier onset of ice melting. Temperature anomalies in the 0–50 m layer at standard stations along the Kola Section were either positive or near the climatic norm, confirming the link between ocean warming and sea ice reduction in recent decades.

The water structure along the Kola Section in summer is shaped by interactions between different currents and seasonal ice melt processes. The southern part of the section is significantly influenced by continental runoff. The central part is characterized by a warm upper layer and the presence of cold, saline bottom waters. In the northern part, a zone of interaction between Atlantic and Arctic waters is observed in the area of the Polar Front. During summer, due to sea ice melting, this frontal zone exhibits a stepped salinity structure with two frontal boundaries. The southern haline front corresponds to the Polar Front, while the northern front, associated with the Arctic Frontal Zone, is observed in the surface layer.

The position of the Polar Front in the Barents Sea remains relatively stable across different climatic periods. The thermal and haline components of the frontal zone exhibit seasonal variability, shifting in response to ice edge displacement. During the ice melting period, particularly in winter, the front moves southward, following the ice edge. During ice formation, the frontal zone shifts southward from the Perseus Ridge slope to the Central Bank. Short-term changes in the frontal zone observed in April and May 2023 were primarily associated with atmospheric processes. The northernmost frontal boundary of the Polar Front in the Barents Sea along the Kola Section was located between 48 to 290 km from the ice edge. Temperature gradients ranged from 0.10 to 0.20 °C/km, salinity gradients from 0.012 to 0.025 psu/km, and the frontal zone width did not exceed 55 km.

The comparison of expeditionary data with model results showed that the global product MERCATOR PSY-4QV3R1 provided the closest values for the gradient and the position of characteristic isolines for the frontal zone during the ice formation period (January and November 2023). During the transition period from ice formation to ice melting (April 2023), the regional reanalysis TOPAZ5 most accurately reproduced the variability of temperature and salinity in the Polar Front. To obtain reliable information on the variability of hydrological conditions in frontal zones located in remote Arctic regions with active ice dynamics, a comprehensive approach is necessary, taking into account all available forms of hydrological data. The study evaluated the quality of reanalysis in reproducing temperature and salinity in the Polar Front of the Barents Sea along the Kola Section.

Funding

Funding for the work performed by *T.M. Maksimovskaya, A.V. Zimin, O.A. Atadzhanova, A.A. Konik* was received within the framework of the state assignment of the Ministry of Education and Science of Russia for IO RAS (project No FMWE-2024-0028). Funding for the work performed by *D.V. Moiseev* was received within the framework of the state assignment of the Ministry of Education and Science of Russia for MMBI RAS (project No FMEE-2024-0016).

Финансирование

Финансирование работ, выполненных *Т.М. Максимовской, А.В. Зиминым, О.А. Атаджановой и А.А. Коником*, получено в рамках государственного задания Минобрнауки России для ИО РАН (тема № FMWE-2024-0028). Финансирование работ, выполненных *Д.В. Моисеевым*, получено в рамках государственного задания Минобрнауки России для ММБИ РАН (тема № FMEE-2024-0016).

References

1. Loeng H, Ozhigin V, Ardlandsvik B. Water fluxes through the Barents Sea. *ICES Journal of Marine Science*. 1997;54(3):310–7. doi:10.1006/jmsc.1996.0165 EDN: LEMVTH
2. Lisitsyn AP. *Barents Sea System*. Moscow: GEOS; 2021. (In Russian).
3. Oziel L, Sirven J, Gascard JC. The Barents Sea frontal zones and water masses variability (1980–2011). *Ocean Science*. 2016;12:169–84. doi:10.5194/os-12-169-2016 EDN: WTVWPP
4. Ingvaldsen RB, Loeng H, Asplin L. Variability in the Atlantic inflow to the Barents Sea based on a one-year time series from moored current meters. *Continental Shelf Research*. 2002;22:505–19. doi:10.1016/S0278-4343(01)00070-X EDN: LRWMBV
5. Skagseth O. Recirculation of Atlantic Water in the western Barents Sea. *Geophysical Research Letters*. 2008;35: L11606. doi:10.1029/2008GL033785 EDN: SPTBDX
6. Lundesgaard Ø, Sundfjord A, Lind S, Nilsen F, Renner AHH. Import of Atlantic Water and sea ice controls the ocean environment in the northern Barents Sea. *Ocean Science*. 2022;18:1389–418. doi:10.5194/os-18-1389-2022 EDN: LLLIPU
7. IPCC. Sections. In: Climate Change 2023: Synthesis Report. Contribution of Working Groups I, II, and III to the Sixth Assessment Report of the Intergovernmental Panel on Climate Change. Geneva: IPCC; 2023. p. 35–115. doi:10.59327/IPCC/AR6-9789291691647
8. Kwok R, Cunningham GF, Wensnahan M, Rigor I, Zwally HJ, YiD. Thinning and volume loss of the Arctic Ocean Sea ice cover: 2003–2008. *Journal of Geophysical Research: Oceans*. 2009;114(C7): C07005. doi:10.1029/2009JC005312 EDN: BUZEJS
9. Schweiger A, Lindsay R, Zhang J, Steele M, Stern H, Kwok R. Uncertainty in modeled Arctic Sea ice volume. *Journal of Geophysical Research: Oceans*. 2011;116(C00D06). doi:10.1029/2011JC007084 EDN: KAKDPU
10. Kostianoy AG, Nihoul JCJ., Rodionov VB. *Physical oceanography of the frontal zones in sub-Arctic seas.* 1st ed. Amsterdam: Elsevier Oceanography Series; 2004. Vol. 71.
11. Kolås EH, Baumann TM, Skogseth R, et al. Western Barents Sea circulation and hydrography, past and present. ESS Open Archive. 2023. doi:10.22541/essoar.169203078.81082540/v1
12. Kolås EH, Fer I., Baumann TM. The Polar Front in the northwestern Barents Sea: Structure, variability, and mixing. *Ocean Science*. 2024;20(6):895–916. doi:10.5194/os-20-895-2024 EDN: KAKDPU
13. Polyakov IV, Pnyushkov A, Carmack E. Stability of the Arctic halocline: A new indicator of Arctic climate change. *Environmental Research Letters*. 2018;13(12):125008. doi:10.1088/1748-9326/aaec1e EDN: RVYNMM
14. Årthun M, Eldevik T, Viste E, Drange H, Furevik T, Johnson HL, Keenlyside N.S. Skillful prediction of northern climate provided by the ocean. *Nature Communications*. 2017;8:15875. doi:10.1038/ncomms15875 EDN: YIBKEK
15. Strong C, Foster D, Cherkaev E, Eisenman I, Golden K. On the definition of marginal ice zone width. *Journal of Atmospheric and Oceanic Technology*. 2017;37(7):1565–84. doi:10.1175/JTECH-D-16-0171.1
16. Kostianoy AG, Nihoul JCJ. Frontal zones in the Norwegian, Greenland, Barents and Bering Seas. In: *NATO Science for Peace and Security Series C: Environmental Security*. 2009. p. 171–90. doi:10.1007/978-1-4020-9460-6_13
17. Bekryaev RV, Polyakov IV, Alexeev VA. Role of polar amplification in long-term surface air temperature variations and modern Arctic warming. *Journal of Climate*. 2010;23(14):3888–906. doi:10.1175/2010JCLI3297.1 EDN: OHMENJ
18. Serreze MC., Barry RG. Processes and impacts of Arctic amplification: A research synthesis. *Global Planet Change*. 2011;77(1–2):85–96. doi:10.1016/j.gloplacha.2011.03.004 EDN: OLOJLP
19. Davy R, Chen L, Hanna E. Arctic amplification metrics. *International Journal of Climatology*. 2018;38(12):4384–94. doi:10.1002/joc.5675 EDN: KNEOBE
20. Latonin MM., Bashmachnikov IL., Bobylev LP. The Arctic amplification phenomenon and its driving mechanisms. *Fundamental and Applied Hydrophysics*. 2020;13(3):3–19. doi:10.7868/S2073667320030016 EDN: ZIPPIB
21. Skagseth Ø, Eldevik T, Årthun M, Asbjørnsen H, Lien VS, Smedsrud LH. Reduced efficiency of the Barents Sea cooling machine. *Nature Climate Change*. 2020;10(7):661–6. doi:10.1038/s41558-020-0772-6 EDN: NJTZCO
22. Sweeney AJ., Fu Q, Po-Chedley S, Wang H, Wang M. Internal variability increased Arctic amplification during 1980–2022. *Geophysical Research Letters*. 2023;50. doi:10.1029/2023GL106060 EDN: LGBUCF

23. Trofimov AG. Arctic and Barents Sea ice extent variability and trends in 1979–2022. *Trudy VNIRO*. 2024;197:101–20. (In Russian). doi:10.36038/2307-3497-2024-197-101-120 EDN: RUYLHJ
24. Screen JA, Simmonds I. The central role of diminishing sea ice in recent Arctic temperature amplification. *Nature*. 2010;464:1334–7. doi:10.1038/nature09051
25. Lind S, Ingvaldsen RB, Furevik T. Arctic warming hotspot in the northern Barents Sea linked to declining sea-ice import. *Nature Climate Change*. 2018;8(7):634–9. doi:10.1038/s41558-018-0205-y EDN: YJCOGD
26. Årthun M, Onarheim IH, Dörr J, Eldevik T. The seasonal and regional transition to an ice-free Arctic. *Geophysical Research Letters*. 2021;48(1). doi:10.1029/2020GL090825 EDN: WSSXAN
27. Ivanov VV, Tuzov FK. Formation of dense water dome over the Central Bank under conditions of reduced ice cover in the Barents Sea. *Deep Sea Research Part I: Oceanographic Research Papers*. 2021;175:103590 EDN: PJKYRT doi:10.1016/j.dsr.2021.103590
28. Sumkina AA, Ivanov VV, Kivva KK. Heat budget of the Barents Sea surface in winter. *Lomonosov Geographical Journal*. 2024;(3):123–34. (In Russian). doi:10.55959/MSU0579-9414.5.79.3.10 EDN: VLIIYL
29. Serreze MC, Stroeve J. Arctic sea ice trends, variability and implications for seasonal ice forecasting. Philosophical Transactions of the Royal Society A. 2015;373:20140159. doi:10.1098/rsta.2014.0159 EDN: UPZPGN
30. Stroeve J, Notz D. Changing state of Arctic sea ice across all seasons. Environmental Research Letters. 2018;13:103001. doi:10.1088/1748-9326/aade56 EDN: LWDJZL
31. Lis NA., Egorova ES. Climatic variability of the ice extent of the Barents Sea and its individual areas. Arctic and Antarctic Research. 2022;68(3):234–47. (In Russian). doi:10.30758/0555-2648-2022-68-3-234-247 EDN: GLBVPA
32. Våge S, Basedow SL, Tande KS, Zhou M. Physical structure of the Barents Sea Polar Front near Storbanken in August 2007. Journal of Marine Systems. 2014;130:256–62. doi:10.1016/j.jmarsys.2011.11.019
33. Fer I, Baumann TM, Elliott F, Kolås EH. Ocean microstructure measurements using an MSS profiler during the Nansen Legacy cruise, GOS2020113, October 2020 [Dataset]. Norwegian Marine Data Centre, 2023.
34. Karsakov AL, Trofimov AG, Antsiferov MYu, et al. 120 years of oceanographic observations at the Kola meridian section. Murmansk: PINRO im. N.M. Knipovicha; 2022. (In Russian). EDN: NOCWAT
35. Ozhigin VK, Trofimov AG, Ivshin VA. The Eastern Basin Water and Currents in the Barents Sea. ICES Document CM 2000/L:14. 19 pp. EDN: YWCURA
36. Polyakov IV, Alekseev GV, Timokhov LA, Bhatt US, Colony RL, Simmons HL, Walsh D, et al. Variability of the Intermediate Atlantic Water of the Arctic Ocean over the last 100 years. *Journal of Climate*. 2004;17:4485–95. doi: 10.1175/1520-0442(2004)017. EDN: LINLZV
37. Loeng H. Features of the physical oceanographic conditions of the Barents Sea. In: Pro Mare Symposium on Polar Ecology; Sakshaug E, Hopkins CCE, Britsland NA, Eds. Polar Research. Trondheim, Norway: 1991. Vol. 10, pp. S18.
38. Karsakov AL. Oceanographic investigations along the "Kola Meridian" section in the Barents Sea in 1900–2008. Murmansk: PINRO Press; 2009. 139 pp. (In Russian).
39. Boitsov VD., Karsakov AL., Trofimov AG. Atlantic water temperature and climate in the Barents Sea, 2000–2009. *ICES Journal of Marine Science*. 2012;69:833–40. doi:10.1093/icesjms/fss075 EDN: RGBVJZ
40. Prokopchuk IP, Trofimov AG. Interannual dynamics of zooplankton in the Kola Section of the Barents Sea during the recent warming period. *ICES Journal of Marine Science*. 2019;76(Supplement_1): i10–i12. doi: 10.1093/icesjms/fsz206 EDN: UOETEB
41. Moiseev DV, Zaporozhtsev IF, Maksimovskaya TM, Dukhno GN. Identification of the position of frontal zones on the surface of the Barents Sea according to contact and remote monitoring data (2008–2018). *Arctic: Ecology and Economy*. 2019;2(34):48–63. (In Russian). doi:10.25283/2223-4594-2019-2-48-63 EDN: JHJGVM
42. Gudkovich ZM, Kirillov AA, Kovalev EG, et al. *Fundamentals of the methodology for long-term ice forecasts for Arctic seas*. Leningrad: Gidrometeoizdat; 1972. 348 pp. (In Russian).
43. Mironov EY. *Ice conditions in the Greenland and Barents Seas and their long-term forecast*. St. Petersburg: AANII; 2004. 319 pp. (In Russian).
44. Afanasyeva EV, Alekseeva TA, Sokolova JV, Demchev DM, Chufarova MS, Bychenkov YuD, Devyataev OS. AARI methodology for sea ice chart composition. *Russian Arctic*. 2019;7:5–20. doi:10.24411/2658-4255-2019-10071 EDN: YIIBNO
45. Zhichkin AP. Peculiarities of interannual and seasonal variations of the Barents Sea ice coverage anomalies. *Russian Meteorology and Hydrology*. 2015;40:319–26. doi:10.3103/S1068373915050052 EDN: UGFDFF
46. Spichkin VA. Definition of the major anomaly criterion. In: *Studies of ice conditions in the Arctic seas, calculation and forecasting methods: Proceedings of the AANII*. 1987. Vol. 402, pp. 15–19. (In Russian).
47. Matishov GG., Golubev VA., Zhichkin AP. Temperature anomalies in the Barents Sea during summer periods of 2001–2005. *Doklady Earth Sciences*. 2007;412:82–4. doi:10.1134/S1028334X07010187 EDN: MWRBHZ

48. Matishov G, et al. Climate and cyclic hydrobiological changes of the Barents Sea from the twentieth to twenty-first centuries. *Polar Biology*. 2012;35:1773–90. doi:10.1007/s00300-012-1237-9 EDN: PVITCJ
49. Fedorov KN. *The physical nature and structure of oceanic fronts.* New York, NY, USA: Springer-Verlag; 1986. 333 pp. doi:10.1007/978-1-4684-6343-9
50. Journel AG, Huijbregts C. *Mining geostatistics.* San Diego, CA, USA: Academic Press; 1978. 600 pp.
51. Dukhovskoy DS, et al. Skill metrics for evaluation and comparison of sea ice models. *Journal of Geophysical Research: Oceans*. 2015;120:5910–31. doi:10.1002/2015JC010989 EDN: VEUXNX
52. Hiester HR, et al. A topological approach for quantitative comparisons of ocean model fields to satellite ocean color data. *Methods in Oceanography*. 2016;13:1–14. doi:10.1016/j.mio.2016.01.001
53. Thomson RE, Emery WJ. *Data analysis methods in physical oceanography.* Newnes; 2014. 638 pp. doi:10.1016/C2010-0-66362-0 EDN: VFCGLJ
54. Efstathiou E, Eldevik T, Årthun M, Lind S. Spatial patterns, mechanisms, and predictability of Barents Sea ice change. *Journal of Climate*. 2022;35:2961–73. doi:10.1175/JCLI-D-21–0044.1 EDN: BPVZBU
55. Årthun M, Eldevik T, Smedsrud L, Skagseth Ø, Ingvaldsen R. Quantifying the influence of Atlantic heat on Barents Sea ice variability and retreat. *Journal of Climate*. 2012;25:4736–43. doi:10.1175/JCLI-D-11-00466.1 EDN: RPHDXJ
56. Herbaut C, Houssais MN, Close S, Blaizot AC. Two wind-driven modes of winter sea ice variability in the Barents Sea. *Deep-Sea Research Part I: Oceanographic Research Papers.* 2015;106:97–115. doi:10.1016/j.dsr.2015.10.005 EDN: VEZTNH

About the authors

TATYANA M. Maksimovskaya, Junior Researcher, Shirshov Institute of Oceanology of RAS; Junior Research Associate, Murmansk Marine Biological Institute of RAS, ORCID: 0000-0001-9136-6670, Scopus AuthorID: 57735699200, WoS ResearcherID: AAZ-6535-2020, e-mail: maximovskaja.t@yandex.ru

ALEXEY V. Zimin, Principal Researcher, Shirshov Institute of Oceanology of RAS, DrSc (Geogr.), ORCID: 0000-0003-1662-6385, Scopus AuthorID: 55032301400, WoS ResearcherID: C-5885–2014, e-mail: zimin2@mail.ru

OKSANA A. Atadzhanova, Senior Researcher, Shirshov Institute of Oceanology of RAS, CandSc (Geogr.), ORCID: 0000-0001-6820-0533, Scopus AuthorID: 57188718743, WoS ResearcherID: R-7835–2018, e-mail: oksanam07@list.ru

ALEXANDER A. Konik, Researcher, Shirshov Institute of Oceanology of RAS, CandSc (Geogr.), ORCID: 0000-0002-2089-158X, Scopus AuthorID: 57203864647, WoS ResearcherID: AAB-7195–2020, e-mail: konikrshu@gmail.com

ELIZAVETA S. Egorova, Lead Specialist, Lomonosov Moscow State University Marine Research Center, CandSc (Geogr.), ORCID: 0000-0001-7207-6002, Scopus AuthorID: 57964657200, WoS ResearcherID: JRX-1701–2023, e-mail: e.egorova@marine-rc.ru

DENIS V. Moiseev, Deputy Director for Science, Murmansk Marine Biological Institute of RAS, CandSc (Geogr.), ORCID: 0000-0003-0141-374X, Scopus AuthorID: 35069960500, WoS ResearcherID: C-1651–2015, e-mail: denis_moiseev@mmbi.info